GA–A22575

FAST WAVE CURRENT DRIVE IN NEUTRAL BEAM HEATED PLASMAS ON DIII–D

by

C.C. PETTY, C.B. FOREST, R.I. PINSKER, J.S. deGRASSIE,
F.W. BAITY, R.W. CALLIS, W.P. CARY, S.C. CHIU, R.L. FREEMAN,
P. GOHIL, R.J. GROEBNER, H. IKEZI, E.F. JAEGER, Y.R. LIN-LIU,
M. MURAKAMI, M. PORKOLAB, R. PRATER, and B.W. RICE

APRIL 1997

GA–A22575

FAST WAVE CURRENT DRIVE IN NEUTRAL BEAM HEATED PLASMAS ON DIII–D

by

C.C. PETTY, C.B. FOREST, R.I. PINSKER, J.S. deGRASSIE, F.W. BAITY,[1] R.W. CALLIS, W.P. CARY, S.C. CHIU, R.L. FREEMAN, P. GOHIL, R.J. GROEBNER, H. IKEZI, E.F. JAEGER,[1] Y.R. LIN-LIU, M. MURAKAMI,[1] M. PORKOLAB,[2] R. PRATER, and B.W. RICE[3]

This is a preprint of an invited paper presented at the 12th Topical Conference on Radio Frequency Power in Plasmas, April 1–3, 1997, Savannah, Georgia, and to be printed in the *Proceedings.*

Work supported by U.S. Department of Energy Contracts DE-AC03-89ER51114, DE-AC05-96OR22464, and W-7405-ENG-48

[1]Oak Ridge National Laboratory
[2]Massachusetts Institute of Technology
[3]Lawrence Livermore National Laboratory

GENERAL ATOMICS PROJECT 3466
APRIL 1997

Fast Wave Current Drive in Neutral Beam Heated Plasmas on DIII–D

C.C. Petty, C.B. Forest, R.I. Pinsker, J.S. deGrassie,
F.W. Baity,[1] R.W. Callis, W.P. Cary, S.C. Chiu
R.L. Freeman, P. Gohil, R.J. Groebner, H. Ikezi,
E.F. Jaeger,[1] Y.R. Lin-Liu, M. Murakami,[1] M. Porkolab,[2]
R. Prater, and B.W. Rice[3]

General Atomics, San Diego, California 92186

Abstract. The physics of non-inductive current drive and current profile control using the fast magnetosonic wave has been demonstrated on the DIII–D tokamak. In non-sawtoothing discharges formed by neutral beam injection (NBI), the radial profile of the fast wave current drive (FWCD) was determined by the response of the loop voltage profile to co, counter, and symmetric antenna phasings, and was found to be in good agreement with theoretical models. The application of counter FWCD increased the magnetic shear reversal of the plasma and delayed the onset of sawteeth, compared to co FWCD. The partial absorption of fast waves by energetic beam ions at high harmonics of the ion cyclotron frequency was also evident from a build up of fast particle pressure near the magnetic axis and a correlated increase in the neutron rate. The anomalous fast particle pressure and neutron rate increased with increasing NBI power and peaked when a harmonic of the deuterium cyclotron frequency passed through the center of the plasma. The experimental FWCD efficiency was highest at 2 T where the interaction between the fast waves and the beam ions was weakest; as the magnetic field strength was lowered, the FWCD efficiency decreased to approximately half of the maximum theoretical value.

INTRODUCTION

Non-inductive control of the steady-state current profile is required to achieve the enhanced confinement and stability properties desired in a tokamak plasma. One key tool in this effort on DIII–D is fast wave current drive (FWCD), which provides a means of control for the central current density profile. The FWCD

[1]Oak Ridge National Laboratory, Oak Ridge, Tennessee 37831.
[2]Massachusetts Institute of Technology, Cambridge, Massachusetts 02139.
[3]Lawrence Livermore National Laboratory, Livermore, California 94551.

system complements the electron cyclotron heating (ECH) system, which can provide off-axis non-inductive current drive. Ongoing FWCD experiments on DIII–D are aimed at demonstrating current profile control and (ultimately) maintaining stationary current profiles that improve the tokamak performance.

Previous experiments on DIII–D have established a firm foundation for the physics of central electron heating [1] and current drive [2,3] with fast waves. Electrons can absorb the fast wave through the coherent combination of Landau damping and transit time magnetic pumping [4,5]. Full non-inductive current drive has been achieved on DIII–D using a single four-strap fast wave antenna in combination with ECH [6].

Three FWCD systems are now operational on DIII–D, each of which consists of a four-strap antenna and a 2 MW radiofrequency (RF) generator. For the experiments reported in this paper, one antenna was tuned to 60 MHz while the other two antennas were operated at 83 MHz; these frequencies correspond to 4–7 times the deuterium cyclotron frequency. The antennas utilized 90° toroidal phasing between straps to launch a directional wave; the phasing could be changed from co to counter current drive between discharges. Non-current drive phasings were also possible either by using a symmetric antenna phasing such as $(0, \pi, \pi, 0)$ or by using co and counter phasings on separate antennas in opposition.

All of the advanced tokamak scenarios proposed for DIII–D utilize neutral beam injection (NBI) heating as well as RF heating. In addition, many of the critical diagnostics on DIII–D such as the motional Stark effect (MSE) and charge exchange recombination (CER) emission require the NBI system. Therefore, it is important to study the physics of FWCD and current profile control in a NBI heated environment on DIII–D. The interaction of the fast waves with the energetic beam ions at high harmonics of the ion cyclotron frequency was also studied in these plasmas. This interaction is analogous to the absorption of FWCD power by the energetic alpha particles in an ignition device.

FWCD MEASUREMENTS

Detailed measurements of the profiles of non-inductive current driven by fast waves on DIII–D permit a stringent comparison between theory and experiment. The non-inductive current profile can be determined from the difference between the measured plasma current profile, obtained from equilibrium reconstructions constrained by MSE data, and the Ohmic current profile; the Ohmic current profile in turn was obtained from the internal parallel loop voltage determined from the time derivative of the poloidal flux and the conductivity profile calculated from the measured plasma profiles [7]. The 16-channel MSE diagnostic was critical to these internal loop voltage measurements. The neutral beams were injected during the current ramp phase and throughout the FWCD pulse to obtain MSE data; the NBI heating had the additional benefit of increasing the target electron temperature to ~ 3 keV which increased the fast wave damping and delayed the onset of sawteeth.

Analysis of six L–mode discharges with NBI heating alone (no FWCD) found that the measured non-inductive current was in good agreement with the expected neutral beam current drive (NBCD) and bootstrap current.

The FWCD radial profile was determined from the change in the noninductive current profile as the antenna phasing was changed from co to counter current drive under otherwise similar conditions. The profiles of the measured internal loop voltages and non-inductive current densities are shown in Fig. 1 for three L–mode plasmas with co, symmetric, and counter antenna phasings. The effect of FWCD on the loop voltage profile is clearly discernible in the central region of the plasma, with the symmetric phasing case lying neatly between the co and counter cases. The non-inductive current density derived from the loop voltage shows a marked dependence on the antenna phasing inside of $r/a = 0.5$; this is the expected region of FWCD. The integrated non-inductive current for the symmetric phasing case agrees with the calculated NBCD and bootstrap current, while the difference between the non-inductive currents for the co and counter phasings indicates that 240 kA of FWCD was present with a centrally peaked profile.

The magnitude and radial profile of the measured FWCD is in good agreement with theoretical models, as found previously on DIII–D [8]. The profile of the non-inductive current density driven by fast waves for co and counter antenna phasings is shown in Fig. 2 for an L–mode plasma with 280 kA of measured FWCD. This figure also shows the theoretical FWCD predictions from the FASTCD model based on the ergodic, weak damping limit [9], the CURRAY ray-tracing model that includes multiple reflections [10], and the PICES reduced full-wave model [11]. Parasitic ion absorption is included in the PICES calculation but is neglected in the FASTCD and CURRAY calculations. The experimental and theoretical FWCD profiles in Fig. 2 are in good agreement, with the measured profile being only slightly broader than the predicted profile. The integrated non-inductive currents from the three models are within 10% of the measured value. Figure 2 also demonstrates that current density driven by fast waves is large compared to the net current density near the plasma axis; therefore, effective current profile modification with the fast waves is possible.

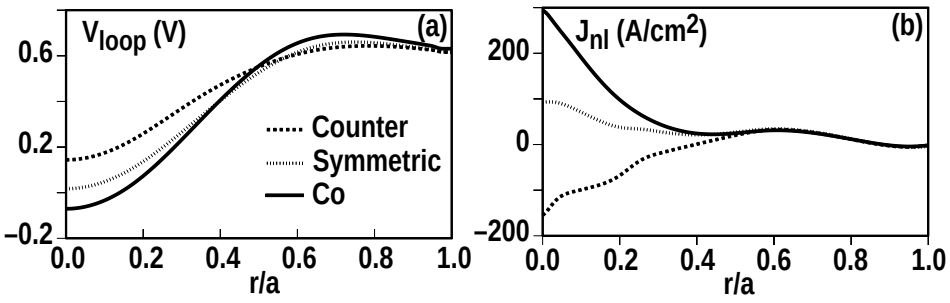

FIGURE 1. Radial profiles of (a) loop voltage and (b) non-inductive current density for three antenna phasings ($B_T = 2.1$ T, $\bar{n} = 1.9 \times 10^{19}$ m^{-3}, $P_{nbi} = 3.7$ MW, $P_{fw} = 2.2$ MW).

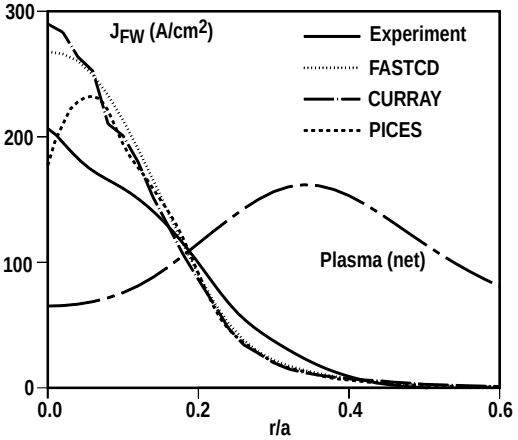

FIGURE 2. Radial profile of the non-inductive current density driven by fast waves along with theoretical profiles. The net plasma current density is also shown for comparison ($B_T = 2.1$ T, $\bar{n} = 2.1 \times 10^{19}$ m^{-3}, $P_{nbi} = 5.0$ MW, $P_{fw} = 2.1$ MW).

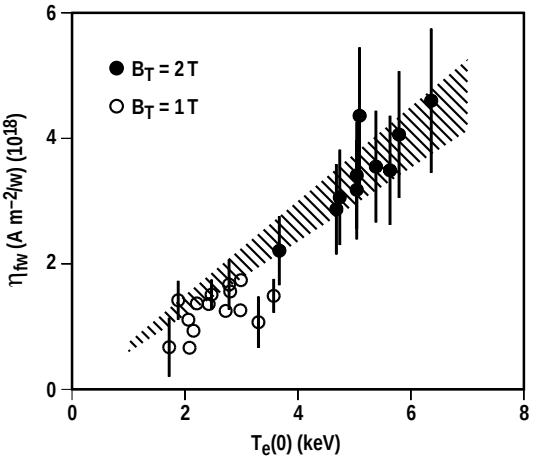

FIGURE 3. Experimental FWCD efficiency as a function of central electron temperature. The shaded band indicates the predictions from the CURRAY ray tracing code.

The measured FWCD efficiency is observed to increase linearly with the electron temperature over a factor-of-4 range, as shown in Fig. 3. The $B_T = 1$ T data were derived from a surface loop voltage analysis [3], while the $B_T = 2$ T data were derived from co/counter comparisons of the internal loop voltages as in Fig. 1. The predicted scaling of the FWCD efficiency from the CURRAY code is also indicated in Fig. 3 by the shaded band, and is found to agree with the experiments. The linear electron temperature dependence projects to attractive current drive efficiencies for power plant conditions.

CURRENT PROFILE CONTROL

The current density driven by the fast waves was comparable to the net current density near the plasma axis, which resulted in substantial current profile modification. Initial experiments on DIII–D found little difference between the current profiles for co and counter FWCD, which was attributed to an offsetting change in the large Ohmic current profile [12]. To mitigate this Ohmic effect, recent experiments in DIII–D at higher RF power have increased the ratio of the FWCD to Ohmic currents by a factor-of-3 or more, which allowed for effective current profile control.

The application of counter FWCD increased the magnetic shear reversal and delayed the onset of sawteeth, compared to co FWCD. Figure 4 shows the central electron temperatures and safety factors for two L–mode discharges with co and counter FWCD (starting at 1000 ms) that were otherwise similar. The central safety factor was substantially raised by counter current drive, which postponed the time of the first sawtooth by 250 ms compared to co current drive. Even after

sawtoothing began, the sawtooth period for the discharge with counter phasing was three times longer than the sawtooth period for co phasing. The current profile control possible with central FWCD is also evident from the change in the net current density and safety factor profiles when switching between co and counter phasings, as shown in Fig. 5. Counter phasing peaked the plasma current off-axis, increased the shear reversal, and moved the location of the minimum in the safety factor to larger radii. These different current profiles produced by co and counter FWCD also exhibited different thresholds for tearing mode activity [13].

BEAM ION ABSORPTION OF FAST WAVES

In parallel with the current drive experiments, the interaction of fast waves with energetic beam ions at high harmonics of the ion cyclotron frequency was studied. The partial absorption of fast waves by beam ions was evident from an anomalously large fast particle pressure near the magnetic axis, as shown in Fig. 6. The total plasma pressure profile was obtained from the magnetic equilibrium reconstruction constrained by the MSE data. For plasmas with NBI heating only, the total pressure profile was in excellent agreement with the sum of the measured thermal and the calculated beam-ion pressure profiles. However, when fast waves were added to the plasma, the total pressure was found to exceed the thermal and calculated beam ion pressure in the central region of the plasma. This anomalous central pressure must come from energetic particles since all of the thermal plasma quantities were measured. In addition, the measured neutron rate (S_n) was substantially greater than the calculated neutron rate (S_{calc}) from beam-thermal and thermonuclear reactions during fast wave injection; the measured and calculated neutron rates were in good agreement for discharges with NBI heating only. The enhanced neutron rate indicates that the anomalous central pressure was due to an energetic deuterium tail on the beam ion distribution caused by ion cyclotron absorption of the fast waves.

The anomalous fast ion pressure and neutron rate peaked when a harmonic of the deuterium cyclotron frequency was located at the center of the plasma. This is shown in Fig. 7, where the anomalous neutron rate $\Delta S_n = S_n - S_{calc}$ and anomalous fast ion stored energy $\Delta W = W_{tot} - W_{th} - W_{beam}$ are plotted for an L–mode magnetic field scan at constant auxiliary power and safety factor. The anomalous stored energy and neutron rate built up over several tenths of a second during the fast wave pulse, which is the source of the spread in ΔS_n and ΔW in Fig. 7 since the data was analyzed at various times with respect to the start of fast wave injection. Figure 7 shows that the largest anomalous neutron rates, of order $\Delta S_n \sim S_n/2$, were obtained when the 6th and 7th harmonics of the deuterium cyclotron frequency for the main FWCD frequency of 83 MHz passed through the plasma center. The anomalous fast ion stored energy, of order $\Delta W \sim W_{tot}/4$, also peaked at the $6\Omega_D$ resonance and showed indications of peaking at the $7\Omega_D$ resonance as well. The amount of fast wave power that was absorbed by the ions can be

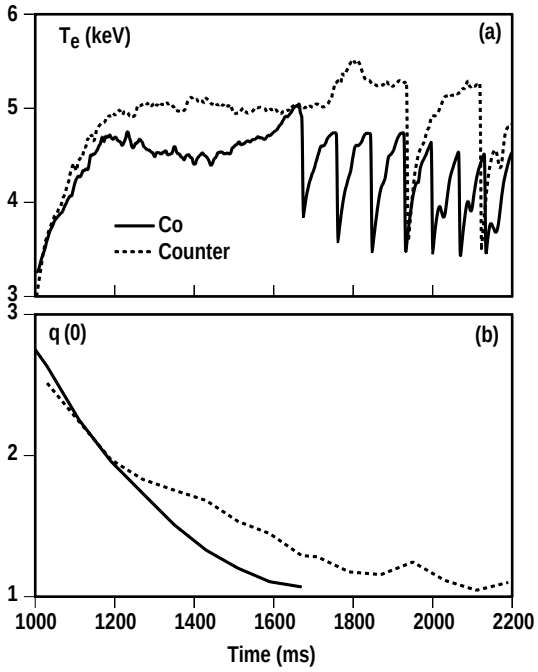

FIGURE 4. Time histories of (a) central electron temperature and (b) central safety factor for matched co and counter FWCD discharges ($B_T = 1.9$ T, $\bar{n} = 1.3 \times 10^{19}$ m^{-3}, $P_{nbi} = 2.6$ MW, $P_{fw} = 2.1$ MW).

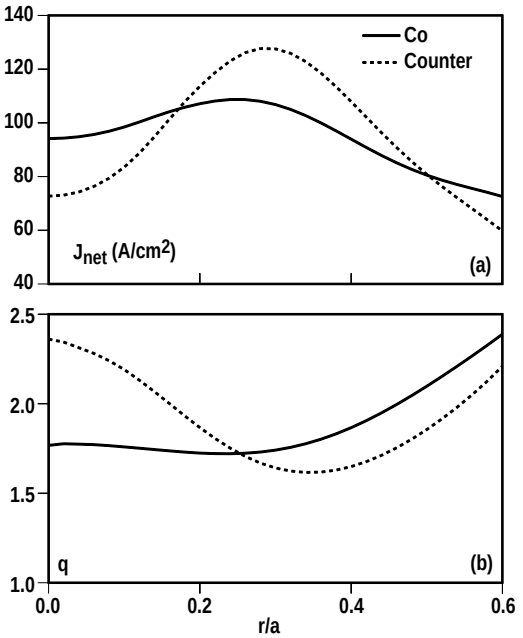

FIGURE 5. Radial profiles of (a) net current density and (b) safety factor at identical times for matched co and counter FWCD discharges ($B_T = 1.9$ T, $\bar{n} = 1.8 \times 10^{19}$ m^{-3}, $P_{nbi} = 3.7$ MW, $P_{fw} = 2.2$ MW).

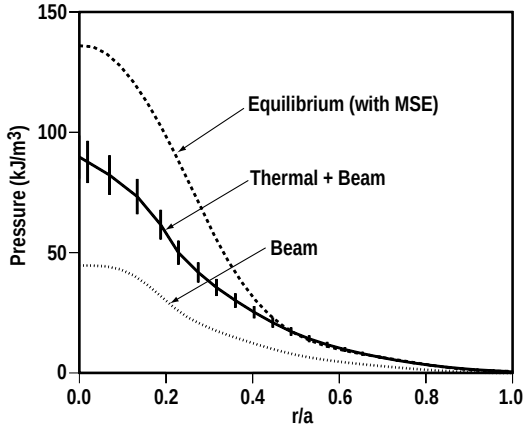

FIGURE 6. Radial profile of the total plasma pressure from a magnetic equilibrium reconstruction, compared to the measured thermal and calculated beam ion pressure profiles. The conditions are the same as for Fig. 5.

estimated from $P_{abs} \approx \Delta W / \tau_s$, where τ_s is the slowing down time of the ion tail. For the case in Fig. 7 where the $6\Omega_D$ resonance passes through the axis of the plasma, this relation gives $P_{abs}/P_{fw} \sim 0.3$ using a calculated value of $\tau_s \approx 0.2$ s

for the plasma center. Modeling of the anomalous neutron rate for this case using the Fokker-Planck code CQL3D [14] also finds that 30% of the FWCD power needs to be absorbed by beam ions to explain the measured neutron rate.

The anomalous neutron rate and fast ion pressure also increased with increasing NBI power, giving further evidence that the fast waves were interacting with the beam ions. An L–mode NBI power scan at constant plasma current and FWCD power is shown in Fig. 8 for a magnetic field where the wave/ion interaction was typically weak. For NBI powers below 4 MW, the anomalous neutron rate and anomalous fast ion stored energy were both relatively small. When the neutral beam power was raised to 5 MW, raising the fast ion beta above 0.5%, a large increase in ΔS_n was observed along with a smaller increase in ΔW. The large increase in ΔS_n relative to ΔW may indicate a change in the dominant ion absorption mechanism from second harmonic damping by the residual hydrogen to 4th and 5th harmonic damping by the beam ions.

The experimental FWCD efficiency was highest at the magnetic field where the interaction between the fast waves and the beam ions was weakest. Figure 9 shows the measured FWCD efficiency, normalized to the central electron temperature, as a function of magnetic field; the theoretical FWCD efficiency calculated by the CURRAY and FASTCD codes assuming no ion absorption is also plotted for comparison. For magnetic

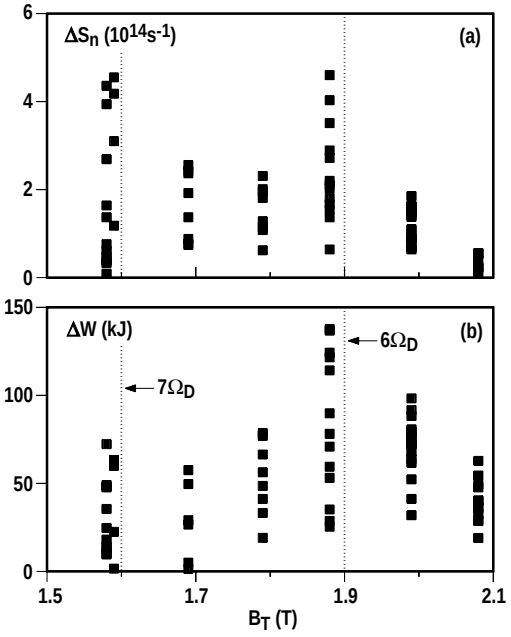

FIGURE 7. Toroidal magnetic field dependence of the (a) anomalous neutron rate and (b) anomalous fast ion stored energy. The magnetic fields for which the 6th and 7th harmonics of the deuterium cyclotron frequency (at 83 MHz) pass through the plasma center are also indicated ($P_{nbi} \approx 3.7$ MW, $P_{fw} \approx 2.3$ MW).

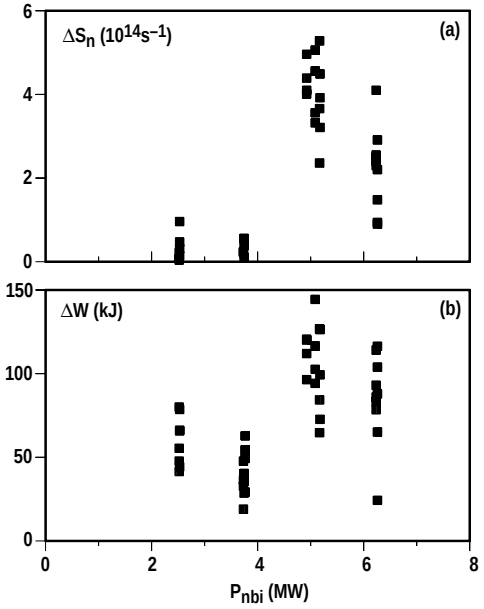

FIGURE 8. Dependence of the (a) anomalous neutron rate and (b) anomalous fast ion stored energy on the neutral beam power ($B_T = 2.1$ T, $\bar{n} = 2.1\times10^{19}$ m^{-3}, $P_{fw} \approx 2.2$ MW).

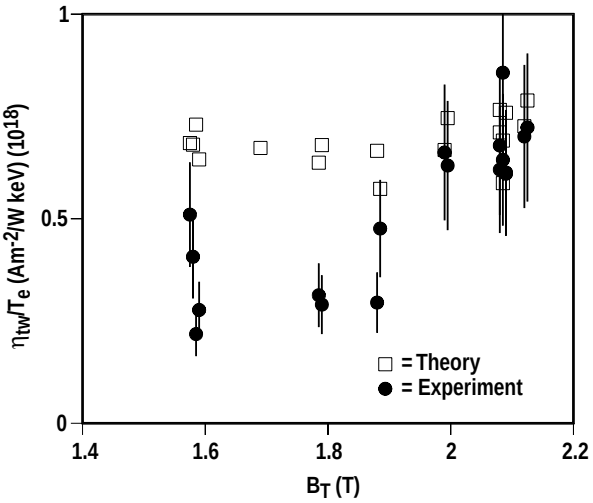

FIGURE 9. Toroidal magnetic field dependence of the FWCD efficiency normalized to the central electron temperature.

fields of 2 T and above, the experimental FWCD efficiency was in good agreement with the maximum efficiency that could be theoretically expected. However, as the magnetic field was lowered, the measured FWCD decreased to approximately half of the maximum theoretical value. The most likely explanation for this is beam ion absorption of the fast waves, which would reduce the amount of power available for current drive. Although the observed absorption of fast waves by beam ions is of the correct magnitude to explain this decrease in the FWCD, the magnetic field dependence of the FWCD efficiency was not as sensitive to the presence of a central deuterium cyclotron harmonic as was the anomalous fast ion pressure or neutron rate (see Fig. 7). This may simply indicate that off-axis ion cyclotron heating does not generate a large energetic tail due to the shorter slowing down time, but further modeling is required to confirm the relationship between the reduced FWCD and the parasitic beam ion absorption.

CONCLUSIONS

Experiments on DIII–D have demonstrated the physics basis for FWCD and current profile control. Partial absorption of the fast waves by the beam ions at high harmonics of the ion cyclotron frequency was observed, which decreased the FWCD efficiency in DIII–D when the magnetic field was below 2 T.

ACKNOWLEDGMENT

This is a report of work sponsored by U.S. Department of Energy Contracts DE-AC03-89ER51114, DE-AC05-96OR22464, and W-7405-ENG-48.

REFERENCES

1. C.C. Petty *et al., Phys. Rev. Lett.* **69**, 289 (1992).
2. R. Prater *et al., Plasma Phys. and Contr. Fusion* **35**, A53 (1993).
3. R.I. Pinsker *et al.*, ''Direct electron heating and current drive with fast waves in DIII–D,'' in *Plasma Physics and Controlled Nuclear Fusion Research* (Proc. 14th Int. Conf. Würzburg, 1992), Vol. 1, p. 109.
4. T.H. Stix, *Nucl. Fusion* **15**, 737 (1975).
5. M. Porkolab, ''On the physics of magnetosonic wave damping on electrons,'' in *Radiofrequency Power in Plasmas* (Proc. 9th Int. Conf. Charleston, 1991), p. 197.
6. C.C. Petty *et al., Nucl. Fusion* **35**, 773 (1995).
7. C.B. Forest *et al., Phys. Rev. Lett.* **73**, 2444 (1994).
8. C.B. Forest *et al., Phys. Plasmas* **3**, 2846 (1996).
9. K. Kupfer, C.B. Forest, C.C. Petty, and R.I. Pinsker, *Phys. Plasmas* **1**, 3915 (1994).
10. T.K. Mau *et al.*, ''Modelling of fast-wave current drive in standard and second-stability bootstrapped reactor plasmas,'' in *Radiofrequency Heating and Current Drive of Fusion Devices* (Proc. 19th Euro. Conf. Brussels, 1992), Vol. 16E, p. 181.
11. E.F. Jaeger *et al., Nucl. Fusion* **33**, 179 (1993).
12. C.C. Petty *et al.*, ''Current profile evolution during fast wave current drive in the DIII–D tokamak,'' in *Radiofrequency Power in Plasmas* (Proc. 11th Int. Conf. Palm Springs, 1995), p. 193.
13. C.B. Forest *et al., Phys. Rev. Lett.* **77**, 3141 (1996).
14. S.C. Chiu *et al.*, ''Interaction of fast waves with ions,'' in *Radiofrequency Power in Plasmas* (Proc. 11th Int. Conf. Palm Springs, 1995), p. 309.